

Large fluctuations and optimal paths in chemical kinetics

M. I. Dykman

Department of Physics, Stanford University, Stanford, California 94305

Eugenia Mori and John Ross

Department of Chemistry, Stanford University, Stanford, California 94305

P. M. Hunt

Department of Chemistry, Michigan State University, East Lansing, Michigan 48824

(Received 10 September 1993; accepted 20 December 1993)

The eikonal approximation (instanton technique) is applied to the problem of large fluctuations of the number of species in spatially homogeneous chemical reactions with the probability density distribution described by a master equation. For both autocatalytic and nonautocatalytic reactions, the analysis of the distribution about a stable stationary state and of the transitions between coexisting stable states comes, to logarithmic accuracy, to the analysis of Hamiltonian dynamics of an auxiliary dynamical system. The latter can be done explicitly in a few cases, including one-species systems, systems with detailed balance, and systems close to the bifurcation points where the number of the stable states changes. In the last case, the fluctuations display universal features, and, for saddle-node bifurcation points, the logarithm of the probability of escape from the metastable state (per unit time) is proportional to the distance to the bifurcation point (in the parameter space) raised to the power $3/2$. We compare the eikonal approximation for the stationary distribution of a master equation to Monte Carlo numerical solutions for two chemical two-variable systems with multiple stationary states, where none of the cited restrictions exists. For one of the systems in the pattern of optimal paths we observe caustics emanating from the saddle point.

I. INTRODUCTION

Chemical systems with ingoing and outgoing flows provide an important class of systems far from thermal equilibrium. For steady external conditions, they can display different types of behavior including the onset of two (or more) stable stationary states and states of persistent oscillations (limit cycles in the space of appropriate variables, e.g., concentrations of species). Fluctuations about the stable states are mostly small, e.g., fluctuations in numbers of molecules are proportional to the square root of these numbers. However, there also occur occasional large fluctuations. These are of particular interest for systems with coexisting stable states, since the transitions between the stable states are due to large fluctuations, and therefore large fluctuations determine which of the dynamically stable states are globally stable and which are metastable. The solution to the problem of large fluctuations also gives the values of the parameters for which the probabilities of the transitions between the states (per unit time) are of the same order of magnitude, so that the populations of the two stable states are of the same order of magnitude and there occurs a "first-order phase transition."

Fluctuations in systems far from thermal equilibrium are usually described on the basis of kinetic equations (cf. Refs. 1 and 2, and references therein). In many cases of interest, in particular, for the reactions in dilute solutions, these equations are Markovian on the time scale "coarse grained" over the duration of an elementary reaction. The theory of large occasional fluctuations in systems described by kinetic equations was first considered by Kramers³ in the context of chemical reaction rates for a simple dynamical system per-

forming Brownian motion in a double-well potential. The statistical distribution of such a system inside a potential well is Gibbsian, and the probability W of the escape from the well per unit time is given by the Arrhenius law $W \propto \exp(-\Delta U/T)$, where ΔU is the well depth and T is the temperature in energy units. Kramers found both the exponent and (what was more complicated) the prefactor for W in a broad range of parameters.

In the general case of a system far from thermal equilibrium, the problem of primary interest is to find the *logarithm* of the statistical distribution, which is in some sense analogous to the thermodynamic potential, and also to find the *logarithm* of the escape probability. The solution to these problems for noise-driven dynamical systems has been obtained first for the noise being white and Gaussian, so that the kinetics is described by a Fokker-Planck equation without detailed balance,⁴⁻¹⁰ and more recently for Gaussian noise with a nonflat power spectrum (Lorentzian peak at zero frequency¹¹ and nonmonotonic spectrum¹²). Chemical kinetics is described by master equations rather than by Fokker-Planck equations. The results immediately related to the issue of the present paper have been obtained in a series of interesting papers.¹³ Matkowsky *et al.*^{13(a)} considered Markov jump processes which were described by difference (over time) rather than differential stochastic equations, so that the kinetics is described by a Kramers-Moyal equation whereas Hu^{13(b)} considered the kinetics described by master equation. The kinetics of Markov systems with discrete time (noisy maps) was analyzed in Ref. 14, with account taken of some features of the dynamics in the absence of noise related specifically to the discreteness of time. The problem of large

fluctuations for Markov chains was considered by Wentzell,¹⁵ Maier has suggested the interesting application of the results to some problems of computer science, where the total probability per unit time of a jump is independent of the state of a system.¹⁶ In the context of chemical kinetics of *multicomponent* systems, the stationary non-Gaussian solution of the master equation for spatially homogeneous non-autocatalytic reactions has been obtained in Ref. 17, and the generalization of this solution to the case of autocatalytic reactions on the basis of some general arguments has been discussed recently.¹⁸

In the present paper, we investigate the probabilities of large occasional fluctuations and the transition probabilities in spatially homogeneous autocatalytic multicomponent systems. The approach is based on the eikonal [or the Wentzel-Kramers-Brillouin (WKB)] approximation as applied to master equations for macroscopic systems. The WKB approximation is advantageous wherever the quantity of interest is fast oscillating (as a wave function of a highly excited state of a quantum system in the classically available range) or fast decaying (as a wave function in the classically forbidden range); in the case under investigation, it is the probability distribution that steeply falls away from the stable state. In Sec. II, the problem of large fluctuations is reduced, to logarithmic accuracy, to a first-order partial differential equation with the appropriate boundary conditions. The concept of the optimal path is discussed, along which the system evolves, with an overwhelming probability, in the course of a large fluctuation to a given point remote from the stable state in the phase space. In Sec. III, the solution of this equation is considered for two simple situations and the results are compared with those obtained by other methods. In Sec. IV, the problem of transition probability is discussed briefly. In Sec. V, the analysis is applied to systems that are close to bifurcation points where the number of the stable stationary states of a system changes. A system is "soft" in the vicinity of a bifurcation point, and fluctuations about a metastable state increase sharply as the parameters approach the bifurcational values where the state disappears. The fluctuations display universal features that depend on the type of bifurcation. Two general types of bifurcation points are considered—saddle-node, where a stable stationary state merges with an unstable one, and spinode bifurcation points (bifurcations of codimension 2), where two stable states and an unstable stationary state merge together. In Sec. VI, the results of the theoretical analysis are applied to chemical kinetics, and the optimal paths and statistical distributions are evaluated numerically for the Selkov model and a two-reactor iodate arsenous acid reaction model. Monte Carlo simulations are presented for these models and the results of the two approaches are compared. In Sec. VII, the main results are summarized and some directions of future work are discussed briefly.

II. EIKONAL APPROXIMATION IN THE PROBLEM OF LARGE FLUCTUATIONS

We consider a set of reagents $i = 1, \dots, M$ in a homogeneous reactor with stationary external constraints such as inflows and outflows. Due to reactions between the species,

their numbers X_1, \dots, X_M ($X_i \geq 1$) evolve in time. Since collisions (and thus the reactions) happen at random, this evolution is a random process, and for dilute systems, this process is Markovian; it is described by a master equation

$$\frac{\partial P(\mathbf{X}, t)}{\partial t} = \sum_{\mathbf{r}} [W(\mathbf{X}-\mathbf{r}, \mathbf{r})P(\mathbf{X}-\mathbf{r}, t) - W(\mathbf{X}, \mathbf{r})P(\mathbf{X}, t)],$$

$$\mathbf{X} \equiv (X_1, \dots, X_M). \quad (1)$$

The function $P(\mathbf{X}, t)$ is the probability density for the system to be in the state with the numbers of species \mathbf{X} at the instant t . It depends on the initial state of the system, or on its initial distribution; in particular, if at the instant $t_0 < t$ the numbers of the species are \mathbf{X}_0 , then the initial condition for Eq. (1) is $P(\mathbf{X}, t_0) = \delta_{\mathbf{X}, \mathbf{X}_0}$. The function $W(\mathbf{X}, \mathbf{r})$ is the probability of the transition $\mathbf{X} \rightarrow \mathbf{X} + \mathbf{r}$ [i.e., of the transition $(X_1, \dots, X_M) \rightarrow (X_1 + r_1, \dots, X_M + r_M)$] per unit time. The values of r_i show the changes in the numbers of the species due to elementary reactions.

The characteristic width of the distribution $P(\mathbf{X}, t)$ is usually very much smaller than the average instantaneous numbers of the species $\mathbf{X}_{\text{det}} \equiv \mathbf{X}_{\text{det}}(t)$. Both the latter and the values of the probabilities W are proportional to the volume of the system Ω , whereas the characteristic fluctuations of X_i scale as $\Omega^{1/2}$ (we will be interested in larger fluctuations, in fact, but still the characteristic values of X_i will be of order Ω). With the neglect of fluctuations, the evolution of the average numbers of the species is described by a deterministic equation which, when written in terms of the probabilities W , is seen from Eq. (1) to be of the form

$$\frac{d\mathbf{X}_{\text{det}}}{dt} = \sum_{\mathbf{r}} \mathbf{r} W(\mathbf{X}_{\text{det}}, \mathbf{r}). \quad (2)$$

The deterministic chemical kinetics is described more often in terms of the total rates $\mathbf{t}^{\pm}(\mathbf{X}, \mathbf{r})$ of the elementary reactions of the birth (t_i^+) and death (t_i^-) of the species i ,^{17,18}

$$\frac{d\mathbf{X}_{\text{det}}}{dt} = \sum_{\mathbf{r}} [\mathbf{t}^+(\mathbf{X}_{\text{det}}, \mathbf{r}) - \mathbf{t}^-(\mathbf{X}_{\text{det}}, \mathbf{r})] \quad [(X_i)_{\text{det}} \geq 1]. \quad (3)$$

The expression for W in terms of \mathbf{t}^{\pm} is of the form

$$W(\mathbf{X}, \mathbf{r}) = \sum_{i(r_i \neq 0)} [t_i^+(\mathbf{X}, \mathbf{r}) - t_i^-(\mathbf{X}, \mathbf{r})] / r_i. \quad (4)$$

The rates t_i^+ and t_i^- are equal to zero for negative and positive r_i , respectively, and therefore the probabilities W as given by Eq. (4) are positive (the values of W do not generally yield the individual t_i^{\pm}).

The stable solutions (attractors) of Eq. (2) give the numbers of the species in the stable states of the system. In the present paper, we assume the attractors to be stationary states $\mathbf{X}_{\text{st}}^{(n)}$, i.e., nodes or foci in the space of the variables \mathbf{X} . With

the neglect of fluctuations, the system placed initially within a basin of attraction of an n th stable state approaches this state in the characteristic relaxation time t_{rel} equal to the reciprocal minimal real part of the eigenvalues of the matrix $\hat{\Lambda}^{(n)}$,

$$\Lambda_{ij}^{(n)} = - \sum_{\mathbf{r}} r_i [\partial W(\mathbf{X}, \mathbf{r}) / \partial X_j]_{\mathbf{X}_{\text{st}}^{(n)}},$$

$$\sum_{\mathbf{r}} \mathbf{r} W(\mathbf{X}_{\text{st}}^{(n)}, \mathbf{r}) = 0. \quad (5)$$

Since both the numbers X_i and the probabilities $W(\mathbf{X}, \mathbf{r})$ are proportional to the volume of the system Ω for $\mathbf{X} = \mathbf{X}_{\text{det}}$, the matrix $\hat{\Lambda}^{(n)}$ is independent of Ω . Due to fluctuations, the evolution of the system on its way to the stable state differs from that described by Eq. (2); however, for large systems, the random trajectories $\mathbf{X}(t)$ form a narrow tube around $\mathbf{X}_{\text{det}}(t)$.

Once an n th stable stationary state $\mathbf{X}_{\text{st}}^{(n)}$ is reached, the system fluctuates about it. The characteristic scale of the fluctuations is of the order of $|\mathbf{X}_{\text{st}}^{(n)}|^{1/2} \propto \Omega^{1/2}$ (Ref. 19) [the validity of this general statement for the system under consideration can be seen from Eq. (1)^{1(b)}]. However, occasionally much larger fluctuations also happen that take the system far from the stable state. Their probabilities are small, but these are large fluctuations that form the *tails* of the stationary statistical distribution; in the case of bi- or multistable systems, they give rise to the switching of the system from one stable state to another. Since the switching probabilities are extremely small compared with the reciprocal relaxation time t_{rel}^{-1} , the statistical distribution of the system about a stable state is quasistationary for the times in between t_{rel} and the reciprocal switching probability, and the switching probability itself is determined by this quasistationary distribution in the vicinity of the saddle point of the system. In the present section, we investigate the quasistationary distribution $P^{(n)}(\mathbf{X})$ about the n th stable state $\mathbf{X}_{\text{st}}^{(n)}$.

The equation for the function $P^{(n)}(\mathbf{X})$ is of the form

$$\sum_{\mathbf{r}} [W(\mathbf{X} - \mathbf{r}, \mathbf{r}) P^{(n)}(\mathbf{X} - \mathbf{r}) - W(\mathbf{X}, \mathbf{r}) P^{(n)}(\mathbf{X})] = 0. \quad (6)$$

In fact, Eq. (6) describes the *stationary* distribution of the system. However, the eikonal (instanton) technique we shall be using does not give immediately the stationary distribution throughout the entire space of the variables in the case of multivariable systems without detailed balance; it gives the distribution only within a certain part of the range of attraction to a stable state where the distribution is *quasistationary* (see Secs. IV and VI). We seek the solution of Eq. (6) in the eikonal form

$$P^{(n)}(\mathbf{X}) = C^{(n)} \exp[-S_n(\mathbf{X})], \quad S_n(\mathbf{X}_{\text{st}}^{(n)}) = 0, \quad (7)$$

where $C^{(n)}$ is a normalization constant which is chosen so that the total probability of finding the system within the basin of attraction to the stable state n is equal to 1. It is convenient to set S_n equal to zero at $\mathbf{X} = \mathbf{X}_{\text{st}}^{(n)}$, where the distribution $P^{(n)}$ is maximal.

When substituting Eq. (7) into Eq. (6), we (i) assume $S_n(\mathbf{X})$ to be smooth, and (ii) neglect the second- and higher-order derivatives of S_n over X_i . However, we *do not* assume the first derivatives to be small, i.e., we put

$$S_n(\mathbf{X} + \mathbf{r}) \cong S_n(\mathbf{X}) + (\mathbf{r} \partial / \partial \mathbf{X}) S_n(\mathbf{X}), \quad |\mathbf{r}| \sim 1 \ll |\mathbf{X}|. \quad (8)$$

The approximation (8) is used below to obtain a first-order differential equation for the function $S_n(\mathbf{X})$. The consistency of this approximation will be justified *a posteriori*. It will be seen that, for the solution obtained, the terms dropped in Eq. (8) are of the order of Ω^{-1} . They make the prefactor of the distribution \mathbf{X} dependent. The idea behind approximation (8) can be understood from a simple example of the Poissonian distribution $P_P(X) = \exp(-X + X \ln X) / X!$. For large X , X , the *logarithm* of $P_P(X)$ changes by $\sim \ln(X/X)$ for X changing by 1, and this change is *not small* for X differing noticeably from its average value \bar{X} . At the same time, the second derivative of $\ln[P_P(X)]$ over X is equal to $-X^{-1}$ and is extremely small for large X ; i.e., the approximation (8) holds. We emphasize that since we do not suppose the first derivatives of $S_n(\mathbf{X})$ to be small, the approximation (8) goes far beyond the Gaussian approximation in the master equation and makes it possible to analyze not only the shape of the quasistationary distribution near its maximum, but also the shape of its far tails up to the range where the number of species differs from its value in the stable state by an order of magnitude: $|\mathbf{X} - \mathbf{X}_{\text{st}}^{(n)}| \sim \Omega \gg \Omega^{1/2}$. The probabilities of the fluctuations resulting in such strong deviations in the numbers of species are exponentially small, and so is the value of $P^{(n)}$ for the corresponding \mathbf{X} .

When substituting Eqs. (7) and (8) into Eq. (6), we assume the transition probabilities $W(\mathbf{X}, \mathbf{r})$ to be smooth functions of \mathbf{X} . They are usually polynomials in X_i .^{1,2,19} The characteristic values of the change in the number of species as a result of a reaction r_i are of order 1. Therefore, to the lowest order in Ω^{-1} , we can neglect the difference between $W(\mathbf{X} - \mathbf{r}, \mathbf{r})$ and $W(\mathbf{X}, \mathbf{r})$ in Eq. (6) for $|\mathbf{X}| \sim \Omega$. It is this feature of the transition probabilities that is the prerequisite for the approximation (8) to hold true. To this approximation, the equation for the function $S_n(\mathbf{X})$ takes the form [cf. Ref. 13(b)]

$$H(\mathbf{x}, \partial S_n(\mathbf{x}) / \partial \mathbf{x}) = 0, \quad H(\mathbf{x}, \mathbf{p}) = \sum_{\mathbf{r}} w(\mathbf{x}, \mathbf{r}) [\exp(\mathbf{r} \mathbf{p}) - 1], \quad (9)$$

where

$$\mathbf{x} = \mathbf{X} / \Omega, \quad s_n(\mathbf{x}) = S_n(\mathbf{X}) / \Omega, \quad w(\mathbf{x}, \mathbf{r}) = W(\mathbf{X}, \mathbf{r}) / \Omega \quad (10)$$

are the densities of the species $\mathbf{x} = (x_1, \dots, x_M)$, the density of the logarithm of the quasistationary distribution about a stable state n , and the density of the transition probability, respectively. In deriving Eq. (9), we have made use of the approximation (8), and it is seen from Eq. (9) that if $s_n(\mathbf{x})$ is smooth, Eq. (8) is a good approximation in the limit of large Ω . The terms neglected in Eq. (8) are of the order of Ω^{-1} .

Equation (9) is a first-order partial differential equation for the function $s_n(\mathbf{x})$. It is immediately related to the corresponding equations that describe the *statistical distribution* of

Markov jump processes^{13(a)} and Markov chains with the total probability of a transition per unit time independent of the state of a system.¹⁶ The kinetic equation for the jump processes analyzed in Ref. 13(a) was a Kramers–Moyal differential (over \mathbf{x}) equation, and the expression for the function $H(\mathbf{x}, \mathbf{p})$ was given by an integral over \mathbf{r} instead of the sum over \mathbf{r} in Eq. (9); this integral goes over into a sum for random walk models, in particular, for one-dimensional ($M=1$), one-step ($|r|=1$) random walks considered in Ref. 13(a) in more detail. Another difference between Eq. (9) and the equations considered in Refs. 13(a) and 16 comes from the fact that, for the processes with discrete time considered in these papers, the total probability to change to a different state and to remain in the one occupied initially over a *given* time interval is equal to 1. In the notation of the present paper, this conditions implies

$$\sum_{\mathbf{r}} w(\mathbf{x}, \mathbf{r}) = \text{const},$$

and by scaling time, the constant in this equation can be made equal to 1. Equation (9) can then be written in the form

$$\ln \left[\sum_{\mathbf{r}} w(\mathbf{x}, \mathbf{r}) \exp(\mathbf{r}\mathbf{p}) \right] = 0, \quad (9a)$$

which is equivalent, in fact, to that used in Refs. 15 and 16. In chemical kinetics, the total reaction rate depends on the state of the system, and the condition that the sum of $w(\mathbf{x}, \mathbf{r})$ be constant does not hold. The average frequency of the collisions between the molecules that give rise to chemical reactions depends on the numbers of the species involved. However, Eq. (9) can be written in the form (9a) with $w(\mathbf{x}, \mathbf{r})$ replaced by $w(\mathbf{x}, \mathbf{r})/\sum_{\mathbf{r}'} w(\mathbf{x}, \mathbf{r}')$, and with the account taken of this renormalization, both of them can be used to find the quasistationary probability density. The eikonal approximation for systems described by the master equation was first considered by Kubo *et al.* and by Kitahara²⁰ (these authors did not analyze the problem of *large* fluctuations, i.e., of the tail of the probability density distribution and of fluctuational transitions between coexisting stable states).

The boundary condition for Eq. (9) is seen from Eq. (7) to be

$$s_n(\mathbf{x}_{\text{st}}^{(n)}) = 0, \quad \mathbf{x}_{\text{st}}^{(n)} \equiv \mathbf{X}_{\text{st}}^{(n)}/\Omega. \quad (11)$$

It follows from this condition and from Eqs. (5) and (9) that $s_n(\mathbf{x})$ is quadratic in $\mathbf{x} - \mathbf{x}_{\text{st}}^{(n)}$ near the stable state

$$s_n(\mathbf{x}) \approx \frac{1}{2} \sum_{ij} A_{ij}^{(n)} [x_i - (\mathbf{x}_{\text{st}}^{(n)})_i] [x_j - (\mathbf{x}_{\text{st}}^{(n)})_j], \quad \mathbf{x} \approx \mathbf{x}_{\text{st}}^{(n)}. \quad (12)$$

The matrix $\hat{A}^{(n)}$ is given by the equation

$$\hat{\Lambda}^{(n)} (\hat{A}^{(n)})^{-1} + (\hat{A}^{(n)})^{-1} (\hat{\Lambda}^{(n)})^+ = \hat{K}^{(n)}, \quad (13)$$

$$K_{ij}^{(n)} = \sum_{\mathbf{r}} w(\mathbf{x}_{\text{st}}^{(n)}, \mathbf{r}) r_i r_j.$$

The matrix $\hat{A}^{(n)}$ is positive definite, since the positiveness of the real parts of the eigenvalues of $\hat{\Lambda}^{(n)}$ is the stability condition, and the matrix $\hat{K}^{(n)}$ is positive definite by construc-

tion (13). It is straightforward to express $\hat{A}^{(n)}$ in terms of the matrix $\hat{U}^{(n)}$ that diagonalizes $\hat{\Lambda}^{(n)}$ and in terms of the eigenvalues λ_i of $\hat{\Lambda}^{(n)}$,

$$\begin{aligned} (\hat{A}^{(n)})^{-1} &= \hat{U}^{(n)} \hat{E}^{(n)} [(\hat{U}^{(n)})^+]^{-1}, \\ E_{ij}^{(n)} &= \{ (\hat{U}^{(n)})^{-1} \hat{K}^{(n)} [(\hat{U}^{(n)})^+]^{-1} \}_{ij} / (\lambda_i + \lambda_j^*), \\ (\hat{\Lambda}^{(n)} \hat{U}^{(n)})_{ij} &= \lambda_j U_{ij}^{(n)}. \end{aligned}$$

The normalization constant in Eq. (7) is given in terms of the matrix $\hat{A}^{(n)}$ by the expression

$$C^{(n)} = \det(\hat{A}^{(n)}) / (2\pi\Omega)^{(M/2)}.$$

A. Hamilton equations of motion

A convenient approach to the analysis of the function $s_n(\mathbf{x})$ is based (cf. Refs. 4–16) on noting that Eq. (9) can be considered as a Hamilton–Jacobi equation for the action of an auxiliary system with the coordinate \mathbf{x} and momentum \mathbf{p} that has the Hamiltonian function $H(\mathbf{x}, \mathbf{p})$ and moves with the energy E equal to zero.²¹ Hamilton’s equations of motion for the system (9) are of the standard form

$$\dot{\mathbf{x}} = \sum_{\mathbf{r}} \mathbf{r} w(\mathbf{x}, \mathbf{r}) \exp(\mathbf{r}\mathbf{p}), \quad (14)$$

$$\dot{\mathbf{p}} = - \sum_{\mathbf{r}} [\exp(\mathbf{r}\mathbf{p}) - 1] \partial w(\mathbf{x}, \mathbf{r}) / \partial \mathbf{x},$$

and, in view of Eq. (9), the action is given by the expression

$$s_n(\mathbf{x}(t)) = \int_{t_0}^t dt' \mathbf{p} \dot{\mathbf{x}} \equiv \int_{t_0}^t dt' L(\mathbf{x}, \dot{\mathbf{x}}), \quad (15)$$

where $L(\mathbf{x}, \dot{\mathbf{x}})$ is the Lagrangian of the auxiliary system

$$L(\mathbf{x}, \dot{\mathbf{x}}) = \mathbf{p} \dot{\mathbf{x}} - H(\mathbf{x}, \mathbf{p}), \quad \mathbf{p} \equiv \mathbf{p}(\mathbf{x}, \dot{\mathbf{x}}), \quad L(\mathbf{x}, \dot{\mathbf{x}}) \geq 0. \quad (16)$$

The function $\mathbf{p}(\mathbf{x}, \dot{\mathbf{x}})$ here is given by the first of Eqs. (14). The nonnegativeness of the Lagrangian L in Eq. (16) follows from the positiveness of $w(\mathbf{x}, \mathbf{r})$ and the inequality $q \exp q + 1 - \exp q \geq 0$, where q stands for $\mathbf{r}\mathbf{p}$. For systems with one species, expressions (9) and (16) for the Hamiltonian and Lagrangian of the auxiliary system go over into those obtained by Kubo *et al.*²⁰ if one replaces r , H , and L by $-r$, $-H$, and $-L$, respectively; the difference comes from the difference in the form of the master equation (1) and that used in Ref. 20, and from the fact that $s_n(\mathbf{x})$ as defined in Eqs. (7) and (10) gives the negative of the logarithm of the statistical distribution.

The boundary conditions for Eqs. (14) follow (cf. Refs. 4, 5, and 7) from the underlying picture of the fluctuations. The quasistationary distribution far from a stable state is formed by occasional large fluctuations. Since the probabilities of large fluctuations are extremely small, the value of $P^{(n)}(\mathbf{X})$ is given, to logarithmic accuracy, by the probability of the most “favorable” fluctuation that brings the system to a given point \mathbf{X} from the vicinity of the stable point $\mathbf{X}_{\text{st}}^{(n)}$, where the system spends most of the time. It is just the function $s_n(\mathbf{x})$ that gives this probability, and Eq. (14) describes the path along which the system arrives to a given \mathbf{x} with an overwhelming probability, i.e., the *optimal path* (cf.

Ref. 4). The value of $\mathbf{x}(t_0)$ at the initial instant t_0 when the large fluctuation starts is close to the stable position $\mathbf{x}_{st}^{(n)}$. It follows from the above picture, and also from Eq. (12), that

$$\mathbf{x}(t_0) \rightarrow \mathbf{x}_{st}^{(n)}, \quad \text{for } t_0 \rightarrow -\infty, \quad \mathbf{x}(t) = \mathbf{x}. \quad (17)$$

It is obvious from Eqs. (14)–(17) that the value of $s_n(\mathbf{x})$ evaluated along the optimal path defined this way is independent of time t , which is consistent with the fact that we consider a *quasistationary* distribution of the system and therefore $\partial s_n / \partial t = -H = 0$.

The important consequence of Eqs. (14)–(17) is that $s_n(\mathbf{x})$ is a Liapunov function. From Eqs. (11) and (17), we see that $s_n(\mathbf{x})$ is positive everywhere in the range of definition except at the stable state $\mathbf{x}_{st}^{(n)}$, where $s_n(\mathbf{x}) = 0$. It is straightforward to see also that $s_n(\mathbf{x})$ decreases when $\mathbf{x} = \Omega^{-1}\mathbf{X}$ approaches the stable state along the deterministic path (2) because the change of the action along the deterministic path^{13(b)}

$$\frac{dS_n[\mathbf{X}_{det}(t)]}{dt} = \Omega \sum_{\mathbf{r}} [\mathbf{r}\mathbf{p}w(\mathbf{x}, \mathbf{r})]_{det} \equiv \Omega \sum_{\mathbf{r}} \{w(\mathbf{x}, \mathbf{r}) \times [\mathbf{r}\mathbf{p} + 1 - \exp(\mathbf{r}\mathbf{p})]\}_{det} \leq 0. \quad (18)$$

Here, the subscript *det* means that \mathbf{x} is set equal to $\Omega^{-1}\mathbf{X}_{det}$, and we have made use of the relations $\partial s_n(\mathbf{x}) / \partial \mathbf{x} = \mathbf{p}$ and $H(\mathbf{x}, \mathbf{p}) = 0$ [Eq. (9)]. The term in the rectangular brackets in the second line of Eq. (18) becomes zero if $\mathbf{p} = 0$. This condition is met in stationary states only. Indeed, it follows from the analysis of the equations of motion (9) and (14) linearized in the vicinity of a stable stationary state [cf. Eq. (12)] that, in addition to the solutions of Eqs. (9) and (14) that describe the optimal paths and satisfy the boundary conditions (17), there is only one more set of solutions that pass through a stable stationary point $\mathbf{x}_{st}^{(n)}$. It corresponds to the deterministic paths, and along them $\mathbf{p} = 0$ and $\mathbf{x}(t) = \mathbf{X}_{det}(t) / \Omega$. At the same time, the dynamical trajectories (9) and (14) can intersect each other in singular points only, and for the motion described by a nonsingular (for finite \mathbf{x} and \mathbf{p}) Hamiltonian function (9), these are fixed points that are singular (we do not consider other possibilities in the present paper). Hence, away from stationary points, we have $\mathbf{p} = \partial s_n(\mathbf{x}) / \partial \mathbf{x} \neq 0$ on the optimal path. Thus, the decrease of the function $s_n(\mathbf{x})$ for \mathbf{x} approaching $\mathbf{x}_{st}^{(n)}$ along the deterministic path is *monotonic*, and $s_n(\mathbf{x})$ is minimal (equal to zero) in the n th stable state itself. This is similar to the behavior of the logarithm of the quasistationary distribution of systems described by a Fokker–Planck equation.⁸

III. OPTIMAL PATHS AND STATISTICAL DISTRIBUTIONS FOR PARTICULAR SYSTEMS

A. Detailed balance and time-inversion problem

A simple expression for the quasistationary and stationary distribution $P^{(n)}(\mathbf{X})$ can be obtained from the master

equation (6) in the important case where detailed balance conditions hold,^{1,2} i.e.,

$$W(\mathbf{X}, \mathbf{r})P^{(n)}(\mathbf{X}) = W(\mathbf{X} + \mathbf{r}, -\mathbf{r})P^{(n)}(\mathbf{X} + \mathbf{r}).$$

This condition implies a relation between the transition probabilities $W(\mathbf{X}, \mathbf{r})$ with the different “jump lengths” \mathbf{r} . In particular, it means that the *ratio* of the probabilities of the “direct” forward and backward transitions $\mathbf{X} \rightarrow \mathbf{X} + \mathbf{r}$ and $\mathbf{X} + \mathbf{r} \rightarrow \mathbf{X}$ is equal to the ratio of the probabilities of the corresponding transitions via intermediate state(s) $\mathbf{X} \rightarrow \mathbf{X} + \mathbf{r}' \rightarrow \mathbf{X} + \mathbf{r}$ and $\mathbf{X} + \mathbf{r} \rightarrow \mathbf{X} + \mathbf{r}' \rightarrow \mathbf{X}$,

$$\frac{W(\mathbf{X}, \mathbf{r})}{W(\mathbf{X} + \mathbf{r}, -\mathbf{r})} = \frac{W(\mathbf{X}, \mathbf{r}')}{W(\mathbf{X} + \mathbf{r}', -\mathbf{r}')} \frac{W(\mathbf{X} + \mathbf{r}', \mathbf{r} - \mathbf{r}')}{W(\mathbf{X} + \mathbf{r}, -\mathbf{r} + \mathbf{r}')}$$

When the detailed balance condition holds, the equation for the function $s_n(\mathbf{x})$ that gives the probability distribution to logarithmic accuracy takes on the form

$$\frac{w(\mathbf{x}, \mathbf{r})}{w(\mathbf{x}, -\mathbf{r})} = \exp \left[-\mathbf{r} \frac{\partial s_n(\mathbf{x})}{\partial \mathbf{x}} \right]. \quad (19)$$

The solution of this equation is trivial and we do not give it. An important consequence of Eq. (19) is that in systems displaying detailed balance, the evolution of the variables $\mathbf{x} = (x_1, \dots, x_M)$ on the optimal path (14) follows just time-inverted evolution for the deterministic path (2)

$$\dot{\mathbf{x}} = - \sum_{\mathbf{r}} \mathbf{r} w(\mathbf{x}, \mathbf{r}) \equiv -\dot{\mathbf{x}}_{det} \quad (20)$$

(cf. Ref. 17).

In the general case, relation (20) does not hold. In a sense, the lack of detailed balance brings time irreversibility into the dynamics of the auxiliary system (14) similar to that brought by a magnetic field into Hamiltonian dynamics.²¹ To see this, one can make a canonical transformation to a new momentum $\boldsymbol{\pi}$ in Eqs. (9), (14), and (15)

$$\mathbf{p} \rightarrow \boldsymbol{\pi}, \quad \boldsymbol{\pi} = \mathbf{p} - \frac{1}{2} \frac{\partial s_n(\mathbf{x})}{\partial \mathbf{x}}$$

The transformation of this type is used to analyze the eigenvalues of a Fokker–Planck equation in continuous Markov systems with detailed balance.^{22,23} It follows from Eq. (19) that, for chemical systems with detailed balance,

$$H(\mathbf{x}, \boldsymbol{\pi}) = H(\mathbf{x}, -\boldsymbol{\pi}), \quad (21)$$

i.e., the Hamiltonian is *even* in the new momentum $\boldsymbol{\pi}$, whereas for systems without detailed balance property (21) does not hold, i.e., dynamics is irreversible in the general case.

B. One-species systems

The equations of motion are greatly simplified if there is only one species involved in the reactions, i.e., the vectors \mathbf{x} and \mathbf{r} have only one component x and r . In this case, Eq. (9) becomes just an algebraic equation for the variable $\exp p$,

$$\sum_r w(x,r)[(\exp p)^r - 1] = 0, \quad (22)$$

which gives immediately p as a function of x ,¹³ and therefore

$$s_n(x) = \int_{x_{st}^{(n)}}^x dx p(x). \quad (23)$$

In the case of the reactions where the number of the species changes by 1, e.g., $A + (m-1)X \rightleftharpoons mX$, detailed balance holds, and Eqs. (22) and (23) give a well-known result

$$\begin{aligned} s_n(x) &= \int_{x_{st}^{(n)}}^x dx \ln[w(x,-1)/w(x,1)] \\ &\equiv \int_{x_{st}^{(n)}}^x dx \ln[t^-(x)/t^+(x)], \end{aligned} \quad (24)$$

where $t^\pm(x)$'s are the total reactive fluxes for a given density x (see Refs. 2 and 24 for a review). In the case of a one-variable Markov process, where the value of the variable changes by ± 1 in an elementary process, the stationary distribution and the problem of the transitions between coexisting stable states were considered by Landauer²⁵ in the context of fluctuations in bistable tunnel diodes.

When the number of X can change by 2 or more, as in the case of reactions with short-living intermediates, expressions (22) and (23) can be easily evaluated numerically. Even in this "one-dimensional" case, the optimal path as given by Eq. (14) is *not* a time-inverted deterministic path. This is in contrast with one-variable systems described by a Fokker-Planck equation where the detailed balance holds "automatically."

IV. TRANSITIONS BETWEEN COEXISTING STABLE STATES

Many chemical systems display, for certain values of the constraints (control parameters), bi- and multistability. For given values of the parameters, they remain for a long time in one or another stable macroscopic state depending on how they have been prepared, and there arises hysteresis on varying parameter values.²⁴ Because of fluctuations, a system can switch spontaneously from one stable state to another. The probability of switching is very small; the negative of its logarithm is proportional to the volume of the system, and therefore switching in macroscopic systems occurs inhomogeneously via nucleation.¹⁹ Because of switchings, a system eventually comes to the most "favorable" stable state. In thermal equilibrium systems, such a state corresponds to the absolute minimum of a thermodynamic potential. The absolute value of the logarithm of the probability of switching from this state is much higher than that from the metastable state that corresponds to a local (but not global) minimum of the thermodynamic potential. The analysis of global stability for nonequilibrium systems can be performed on the basis of switching probabilities as well. The "globally stable" state is that for which the logarithm of the escape probability (per unit volume) is larger in absolute value.

The results given in Sec. II make it straightforward to find the switching probabilities for Markovian systems described by a birth-death master equation. This problem was considered by Landauer²⁵ for a one-component system with $r = \pm 1$. Because of the absence of memory, it is sufficient for switching that the system reach the range of attraction to another stable state in the course of a fluctuation. The system will then approach this state with a probability of order unity along the deterministic path (2). Therefore, to logarithmic accuracy, the probability W_{nm} of the direct switching $n \rightarrow m$ from the n th stable state to the m th one is equal to the probability of a transition from the initially occupied stable state n to the separatrix that separates the basins of attraction to this state and the state m . Moreover, it is necessary to find the maximum of this probability with respect to different points on the separatrix.

It follows from the above arguments that the value of $\ln W_{nm}$ is given by the minimal value of $\Omega s_n(x)$ for x lying on the separatrix. The separatrix itself is a trajectory of deterministic motion towards the saddle point x_s , and since $s_n(x)$ is a Liapunov function, it reaches its minimum on the separatrix right in the saddle point (cf. Ref. 7),

$$\ln W_{nm} \approx -\Omega s_n(x_s), \quad \sum_r r w(x_s, r) = 0 \quad (25)$$

{we do not consider special cases where there are several singular points on a separatrix [cf. Ref. 10(a)]}. Equations (14), (15), and (25) reduce the problem of calculating the switching probabilities to a boundary-value problem for ordinary differential equations which can be solved numerically for a particular system. Since the motion along the optimal path gets slowed down in the vicinity of the saddle point

$$p \rightarrow 0, \quad \dot{x} \rightarrow 0 \quad \text{for } x \rightarrow x_s,$$

it is convenient to surround the saddle point x_s by a small area and to seek a trajectory that starts in the vicinity of the stable point $x_{st}^{(n)}$ and arrives into this area. This algorithm is effective in the case of continuous Markov systems in spite of the fact that a caustic can emanate from the saddle point for system (14) without detailed balance.^{10(b)} The application of this algorithm to particular chemical systems will be considered in Sec. VI below.

Given that the characteristic "specific activation energies" $Ts_n(x_s)$ (T is temperature in energy units) of the escapes from the stable states are known, it is straightforward to find the distribution of the system over the stable states. Actually, these quantities are similar to the depths of the wells of thermodynamic potential in thermal equilibrium systems that experience first-order phase transitions (cf. Refs. 7 and 25). In the stationary regime, the system occupies, with an overwhelming probability, that state for which the value of $s_n(x_s)$ is larger. The range of the phase transition corresponds to the values of the parameters of the system where the activation energies are equal to each other. The width of

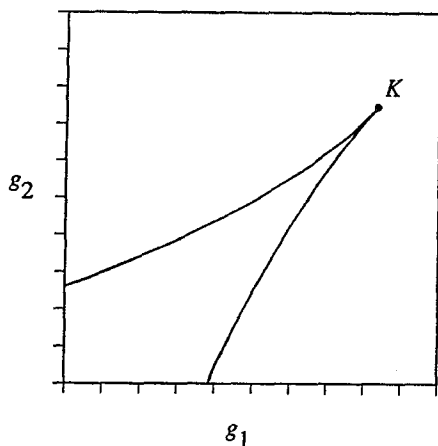


FIG. 1. A schematic form of the bifurcation diagram of a two-parameter system. Inside the "beak," the system has two stable and one unstable stationary states. Smooth lines are the saddle-node bifurcation lines. For the corresponding values of the parameters g_1 and g_2 , one of the stable stationary states merges with the unstable one. In the spinode point K , all stationary states merge together.

this range (in the parameter space) is of order $\Omega^{-1} \ll 1$. Many, but not all phenomena arising in this range in nonequilibrium systems are similar to those known for thermal equilibrium systems.¹⁹

V. STATISTICAL DISTRIBUTION AND ESCAPE PROBABILITIES NEAR BIFURCATION POINTS

The analysis of the form of the probability density distribution is greatly simplified in the range of the constraints (control parameters) close to bifurcation points. We consider two basic types of bifurcations in systems with coexisting stationary states: saddle-node, or marginal bifurcation points (bifurcations of codimension 1), where a stable stationary state of the system merges with an unstable stationary state (a saddle point in the phase space); and spinode bifurcation points (bifurcations of codimension 2), where two stable stationary states and an unstable one merge together.²⁶ The bifurcations of the latter sort occur, generally, in systems with at least two control parameters (e.g., flow densities of two reagents). The bifurcation diagram of a two-parameter system is shown schematically in Fig. 1. The full lines correspond to codimension 1 bifurcations, whereas the spinode point corresponds to the codimension 2 one. Inside the "beak" formed by the curves, a system has two coexisting stable stationary states (in a certain area of the phase space) and an unstable stationary state, and it has only one stable state outside the beak.

In the vicinity of a bifurcation point, a certain type of motion of a dynamical system becomes slow. The slow motion is described effectively by one variable,²⁶ a soft mode. The "softness" of the motion results in a relatively strong response to various perturbations and is expected to result in large fluctuations. A sharp increase of fluctuations and of the probability of escape from a metastable state near bifurcation point has been considered for dynamical systems driven by external noise (see Refs. 27 and 28 and references therein).

This increase is demonstrated in the present section to occur in the case of chemical kinetics too. Moreover, just as in noise-driven dynamical systems, fluctuations in chemical systems near bifurcation points of the deterministic motion have some universal features irrespective of whether there is detailed balance or not.

A. Saddle-node bifurcations

We start with the analysis of fluctuations near a saddle-node (marginal) bifurcation point

$$\mathbf{g} = \mathbf{g}_M, \quad \mathbf{g} \equiv (g_1, g_2, \dots), \quad (26)$$

where g_1, g_2, \dots is the set of the constraints (control parameters of the system). These parameters enter the expressions for the transition probabilities in the master equation (1), i.e.,

$$W(\mathbf{X}, \mathbf{r}) \equiv W(\mathbf{X}, \mathbf{r} | \mathbf{g}), \quad w(\mathbf{x}, \mathbf{r}) \equiv \Omega^{-1} W(\mathbf{X}, \mathbf{r} | \mathbf{g}) = w(\mathbf{x}, \mathbf{r} | \mathbf{g}), \quad (27)$$

and therefore the explicit form of the statistical distribution of the system also depends on \mathbf{g} .

1. Deterministic motion

Bifurcations are the features of the deterministic motion of the system described by the dynamical equation of motion (2). The topology of the trajectories of this equation changes at a bifurcation point. The bifurcation values of the parameters \mathbf{g}_M can be obtained by noticing that in the saddle-node bifurcation point, one of the eigenvalues λ_i of the characteristic matrix $\hat{\Lambda}$ [Eq. (5)] of the stable stationary state that coalesces with the saddle point becomes equal to zero. The resulting equations for the position \mathbf{x}_M of the stationary state itself and for \mathbf{g}_M follow from Eqs. (2) and (27) to be of the form

$$\sum_{\mathbf{r}} \mathbf{r} w(\mathbf{x}_M, \mathbf{r} | \mathbf{g}_M) = 0, \quad \text{Det}(\hat{\Lambda}^{(M)}) = 0, \quad (28)$$

$$\Lambda_{ij}^{(M)} = - \sum_{\mathbf{r}} r_i [\partial w(\mathbf{x}, \mathbf{r} | \mathbf{g}_M) / \partial x_j]_{\mathbf{x}_M}.$$

Equation (28) gives an interrelation between the components g_1, g_2, \dots and thus determines a hypersurface in the parameter space \mathbf{g} ; in the particular case of a two-parameter system, this is just a line on the plane (g_1, g_2) as shown in Fig. 1.

The deterministic motion in the vicinity of a bifurcation point, i.e., for \mathbf{x} and \mathbf{g} close to \mathbf{x}_M and \mathbf{g}_M can be described in the standard way.²⁶ It is convenient to place the origin of the variables and of the control parameters at their values at the bifurcation point and to make a transformation to new variables so as to single out the variable (the combination of the concentrations of the species) which changes slowly in time

$$\mathbf{y} = \hat{U}^{-1}(\mathbf{x} - \mathbf{x}_M), \quad (\hat{U}^{-1} \hat{\Lambda}^{(M)} \hat{U})_{ij} = \lambda_i \delta_{ij}, \quad \lambda_1 = 0. \quad (29)$$

For small $|y_i|$ and $|\mathbf{g} - \mathbf{g}_M|$, the deterministic equation for the slow variable y_1 is of the form

$$\dot{y}_1 \approx \sum_k f_{1k}^{(0)} \delta g_k + \sum_{i,j} f_{1ij}^{(2)} y_i y_j + \dots \quad (\mathbf{y} = \mathbf{y}_{\text{det}}), \quad (30)$$

$$\delta \mathbf{g} = \mathbf{g} - \mathbf{g}_M,$$

whereas the equations for the remaining "fast" variables are

$$\dot{y}_i \approx -\lambda_i y_i + \sum_k f_{ik}^{(0)} \delta g_k + \sum_{i_1, i_2} f_{ii_1 i_2}^{(2)} y_{i_1} y_{i_2} + \dots, \quad i > 1, \quad (31)$$

($\mathbf{y} = \mathbf{y}_{\text{det}}$).

Here we have

$$f_{ik}^{(0)} = \sum_{i_1} (\hat{U}^{-1})_{ii_1} \sum_{\mathbf{r}} r_{i_1} [\partial w(\mathbf{x}, \mathbf{r} | \mathbf{g}) / \partial g_k], \quad (32)$$

$$f_{ijk}^{(2)} = \frac{1}{2} \sum_{i_1, i_2, i_3} (\hat{U}^{-1})_{ii_1} U_{i_2 j} U_{i_3 k} \sum_{\mathbf{r}} r_{i_1} \frac{\partial^2 w(\mathbf{x}, \mathbf{r} | \mathbf{g})}{\partial x_{i_2} \partial x_{i_3}}$$

(all the derivatives are evaluated for $\mathbf{x} = \mathbf{x}_M$, i.e., for $\mathbf{y} = 0$, and $\mathbf{g} = \mathbf{g}_M$).

The relaxation time of the variable y_1 in the stationary state is equal to infinity for $\mathbf{g} = \mathbf{g}_M$ (where $\mathbf{y}_{\text{st}} = 0$). For \mathbf{g} close to \mathbf{g}_M , it is finite, but still it is very much larger than the relaxation times of the other variables which are of the order of $(\text{Re } \lambda_{i>1})^{-1}$. As a result the fast variables $y_{i>1}$ follow the variable y_1 adiabatically. Over a time t that is small enough, so that y_1 remains nearly constant, but is very much larger than $\max(\text{Re } \lambda_{i>1})^{-1}$, they take on their adiabatic stationary values for a given y_1 ,

$$y_i \approx y_i^{(\text{ad})} \equiv y_i^{(\text{ad})}(y_1) \approx \left(\sum_k f_{ik}^{(0)} \delta g_k + f_{i11}^{(2)} y_1^2 \right) / \lambda_i. \quad (33)$$

The deterministic motion of y_1 is given by the equation

$$(\dot{y}_1)_{\text{det}} = \epsilon_M - a_M y_1^2, \quad \epsilon_M = \sum_k f_{1k}^{(0)} \delta g_k, \quad a_M = -f_{111}^{(2)}. \quad (34)$$

It is seen from Eq. (34) that in the range $a_M \epsilon_M > 0$, the system has two coexisting stationary states of deterministic motion, one of them stable \mathbf{y}_{st} and the other unstable (the saddle point) \mathbf{y}_s , and in these states,

$$y_{1\text{st}} = \text{sgn}(a_M) \Delta_M, \quad y_{1s} = -\text{sgn}(a_M) \Delta_M, \quad (35)$$

$$\Delta_M = (\epsilon_M / a_M)^{1/2} \quad (a_M \epsilon_M > 0).$$

The parameter ϵ_M characterizes the distance to the bifurcation point in the parameter space. This parameter is supposed to be small. For $|\epsilon_M| \ll 1$ and for $a_M \epsilon_M > 0$, the relaxation time in the vicinity of the stable state is of the order of Δ_M . It is the inequality

$$\Delta_M \ll \text{Re } \lambda_{i>1} \quad (36)$$

that justifies the adiabatic approximation used above. For

$\epsilon_M = 0$, the stationary states (35) merge together, and for $a_M \epsilon_M < 0$, there are no stable states in the phase space of the system close to \mathbf{x}_M .

2. Optimal paths of fluctuational motion

The slowness of one of the variables of the system (the variable y_1) in the vicinity of a bifurcation point makes it possible to solve the Hamiltonian equations (9) and (14) that give the exponent in expression (7) for the quasistationary probability density distribution. To find the solution, it is convenient to make a canonical transformation to new variables \mathbf{y} and \mathbf{Y} ,

$$\mathbf{y} = \hat{U}^{-1}(\mathbf{x} - \mathbf{x}_M), \quad \mathbf{Y} = \mathbf{p} \hat{U} \left(Y_i \equiv \sum_j p_j U_{ji} \right), \quad (37)$$

where the matrix \hat{U} is defined in Eq. (29). The variables \mathbf{y} and \mathbf{Y} are canonically conjugate coordinates and momenta²¹ of an auxiliary system with the Hamiltonian H' ,

$$\dot{\mathbf{y}} = \frac{\partial H'}{\partial \mathbf{Y}}, \quad \dot{\mathbf{Y}} = -\frac{\partial H'}{\partial \mathbf{y}}, \quad (38)$$

$$H' \equiv H'(\mathbf{y}, \mathbf{Y}) = H(\hat{U} \mathbf{y} + \mathbf{x}_M, \mathbf{Y} \hat{U}^{-1}), \quad H' = 0.$$

The action $s_n(\mathbf{x}) = S_n(\mathbf{X}) / \Omega$ that determines, to logarithmic accuracy, the quasistationary probability density distribution (7) in the vicinity of the metastable state \mathbf{y}_{st} is given by the expression

$$s_M(\mathbf{y}) = \int_{\mathbf{y}_{\text{st}}}^{\mathbf{y}} \mathbf{Y} d\mathbf{y}. \quad (39)$$

Since the variable y_1 is a "soft mode" and the two stationary states are close to each other, we expect the statistical distribution over y_1 to be comparatively flat and strongly non-Gaussian. The characteristic scale for y_1 is given by the small parameter Δ_M [Eq. (35)], whereas the characteristic scale for the variables $y_{i>1}$ is independent of ϵ_M . Therefore, on the scale Δ_M , the distribution over these variables is nearly Gaussian near the maximum. As a whole, to describe the statistical distribution close to \mathbf{y}_{st} , the momentum of the auxiliary system \mathbf{Y} can be assumed to be small and the Hamiltonian function H' can be expanded both in the coordinate \mathbf{y} and momentum \mathbf{Y} (this will be justified *a posteriori*). The lowest-order terms of this expansion are of the form

$$H' \approx \sum Y_i (-\lambda_i y_i + f_{ik}^{(0)} \delta g_k + f_{ijk}^{(1)} y_j \delta g_k + f_{ijj}^{(2)} y_j y_j + f_{ijj}^{(3)} y_j y_j y_j) + \frac{1}{2} \sum F_{ij} Y_i Y_j + \dots \quad (40)$$

Here, the coefficients $f_{ik}^{(0)}$ and $f_{ijk}^{(2)}$ are given in Eq. (32), λ_i 's are the eigenvalues of the matrix $\hat{\Lambda}^{(M)}$ [Eq. (28)] ($\lambda_1 = 0$), and

$$\begin{aligned}
 f_{ijk}^{(1)} &= \sum (\hat{U}^{-1})_{ii_1} \left[\sum_r r_{i_1} \frac{\partial^2 w(\mathbf{x}, \mathbf{r} | \mathbf{g})}{\partial x_{j_1} \partial g_k} \right] U_{j_1 j}, \\
 f_{ijj'j''}^{(3)} &= \frac{1}{6} \sum (\hat{U}^{-1})_{ii_1} \left[\sum_r r_{i_1} \frac{\partial^3 w(\mathbf{x}, \mathbf{r} | \mathbf{g})}{\partial x_{j_1} \partial x_{j'_1} \partial x_{j''_1}} \right] \\
 &\quad \times U_{j_1 j} U_{j'_1 j'} U_{j''_1 j''}, \\
 F_{ij} &= \sum (\hat{U}^{-1})_{ii_1} (\hat{U}^{-1})_{jj_1} \sum_r r_{i_1} r_{j_1} w(\mathbf{x}_M, \mathbf{r} | \mathbf{g}_M).
 \end{aligned} \tag{41}$$

All derivatives in Eq. (41) are evaluated at $\mathbf{x}=\mathbf{x}_M$ and $\mathbf{g}=\mathbf{g}_M$, and the symbol of summation without specification means the sum over repeating indices.

It follows from the equations of motion (38)–(40) that, since $\lambda_1=0$, the components y_1 and Y_1 vary slowly in time [the characteristic time scale for their variation is of the order of Δ_M (see below)], whereas the components $y_{i>1}$ and $Y_{i>1}$ are fast; they vary over the time $\sim |\lambda_{i>1}|^{-1} \ll \Delta_M$. The solution of Eqs. (38) is separated into “fast” and “slow” ones. The slow solution corresponds to the extremum of the function $s_M(\mathbf{y})$ over the variables $y_{i>1}$, i.e., to

$$Y_i = 0, \quad i > 1$$

for a given value of y_1 . The slow motion is effectively one dimensional

$$\begin{aligned}
 Y_1 &= -2F_{11}^{-1}(\epsilon_M - a_M y_1^2), \\
 \dot{y}_1 &= -(\epsilon_M - a_M y_1^2), \quad y_{i>1} = y_{i>1}^{(\text{ad})},
 \end{aligned} \tag{42}$$

where $y_{i>1}^{(\text{ad})} \equiv y_{i>1}^{(\text{ad})}(y_1)$ are given by Eq. (33), and the parameters ϵ_M and a_M are defined in Eq. (34). It follows from Eqs. (35) and (42) that the characteristic time scale for the slow motion is indeed given by Δ_M^{-1} .

The fast solution of Eq. (38) is of the form

$$\begin{aligned}
 Y_i &\approx \sum_{j>1} A_{ij}(y_j - y_j^{(\text{ad})}), \quad \dot{y}_i \approx \lambda_i(y_i - y_i^{(\text{ad})}), \quad i > 1, \\
 (\hat{A}^{-1})_{ij} &= F_{ij}/(\lambda_i + \lambda_j) \quad (i, j > 1).
 \end{aligned} \tag{43}$$

The action in the vicinity of a marginal bifurcation point s_M is given by the expression

$$\begin{aligned}
 s_M(\mathbf{y}) &= \Psi_M(y_1) - \Psi_M(y_{1\text{st}}) \\
 &\quad + \frac{1}{2} \sum_{i,j>1} A_{ij} [y_i - y_i^{(\text{ad})}(y_1)] [y_j - y_j^{(\text{ad})}(y_1)], \\
 \Psi_M(y) &= 2(F_{11})^{-1} (\frac{1}{3} a_M y^3 - \epsilon_M y),
 \end{aligned} \tag{44}$$

$$y_{1\text{st}} = \text{sgn}(a_M) \Delta_M.$$

According to Eq. (44), s_M is parabolic in the fast variables, i.e., their probability density distribution is Gaussian. We note that this is true only near the maximum of the distribution with respect to the fast variables; however, the range is not limited to the close vicinity of the stable state, as in Eq. (12). We have here a Gaussian-shaped “ridge” of the probability density along the y_1 variable. At the same time, the distribution over the slow variable y_1 is strongly non-

Gaussian already for $|y_1 - y_{1\text{st}}| \sim \Delta_M \ll 1$. Its negative logarithm is given by a cubic parabola with a minimum in the stable state $y_{1\text{st}}$ and with a local maximum in the unstable stationary state (the saddle point). The behavior of $s_M(\mathbf{y})$ is generic—the function Ψ_M contains two parameters and can be scaled to a function of one parameter only, this parameter being the square root of the (scaled) distance to the bifurcation point in the parameter space Δ_M ,

$$\Psi_M(y) = 2(F_{11})^{-1} a_M \psi_M(\Delta_M, y/\Delta_M), \tag{45}$$

$$\psi_M(\Delta_M, z) = \Delta_M^3 z (\frac{1}{3} z^2 - 1).$$

It is the smallness of Δ_M that justifies both the adiabatic approximation used above (the separation of variables into fast and slow ones) and the expansion of the Hamiltonian H' in \mathbf{y} and \mathbf{Y} [Eq. (40)]. It follows from Eq. (44) that the “distance” between the minimum and the maximum of the distribution along y_1 is $\sim \Delta_M$, and along $|y_{i>1}^{(\text{ad})}|$ it is $\sim \Delta_M^2$, so that if we are interested in the values of s_M not exceeding greatly these in the saddle point $\Psi_M(y_{1s}) - \Psi_M(y_{1\text{st}})$, it suffices to consider the range $|Y_{i>1}| \leq \Delta_M^{3/2}$.

Close to the saddle-node bifurcation point, the activation energy of escape from the metastable state is given by $\Psi_M(y_{1s}) - \Psi_M(y_{1\text{st}})$. It is proportional to $\Delta_M^3 \propto |\epsilon_M|^{3/2}$, i.e., it scales with the distance to the bifurcation point as $|\epsilon_M|^{3/2}$. This law holds for $|\epsilon_M|$ not too small. It is necessary that s_M be much larger than the reciprocal total number of particles in the system. In the vicinity of a bifurcation point, according to Eqs. (42) and (43), the evolution of the variables along the optimal fluctuation path is just the time-inversed evolution along the deterministic path [Eqs. (31) and (34)]. This result holds *in the absence* of detailed balance in the system as a whole and is related to the one-dimensional character of the fluctuations and to the softness of the system.

B. Fluctuations in the vicinity of a spinode point

The above analysis can be generalized to bifurcations of a higher codimension, in particular, to the bifurcation of codimension 2, where two stable states and a saddle point coalesce together. Such a bifurcation corresponds to a spinode point on the two-branch bifurcation curve that describes saddle-node bifurcations in Fig. 1, and the fluctuations in the vicinity of the spinode point in a spatially uniform chemical system have much in common with the fluctuations at the critical point in systems that experience first-order phase transition as described by the mean-field theory.¹⁹ For the control parameters lying inside the beak, the system has two stable states and an unstable stationary state (the saddle point). The latter one merges with one or the other of the former ones on the branches of the bifurcation curve, whereas in the spinode point, all three stationary states merge together.²⁶ The values of the parameters in the spinode point $\mathbf{g}=\mathbf{g}_K$, and the position of the stationary state \mathbf{x}_K , are given, in terms of the eigenvalues λ_i of the characteristic matrix $\hat{\Lambda}$ [Eq. (5)] and the functions $f^{(2)}$ [Eq. (32)] calculated for $\mathbf{x}=\mathbf{x}_K$ and $\mathbf{g}=\mathbf{g}_K$, by the equations

$$\sum_{\mathbf{r}} \mathbf{r} w(\mathbf{x}_K, \mathbf{r} | \mathbf{g}_K) = 0, \quad \lambda_1 = 0, \quad f_{111}^{(2)} = 0. \quad (46)$$

The deterministic motion in the vicinity of the spinode point can be separated, just as in the case of a saddle-node bifurcation, into a slow one and the remaining fast ones, and, by implying canonical transformation (29) with the matrix \hat{U} evaluated for $\mathbf{g} = \mathbf{g}_K$ and $\mathbf{x} = \mathbf{x}_K$, the equations of motion for $\mathbf{y} = \hat{U}(\mathbf{x} - \mathbf{x}_K)$ can be reduced to a form similar to Eqs. (30) and (31)

$$\begin{aligned} \dot{y}_i = & -\lambda_i(1 - \delta_{i1})y_i + \sum f_{ik}^{(0)} \delta g_k + \sum f_{ijk}^{(1)} y_j \delta g_k \\ & + \sum f_{ijj'}^{(2)} y_j y_{j'} + \sum f_{ijj'j''}^{(3)} y_j y_{j'} y_{j''} + \dots, \\ \mathbf{y} = & \mathbf{y}_{\text{det}}. \end{aligned} \quad (47)$$

The coefficients here are given by Eqs. (32) and (41) with all the derivatives evaluated for $\mathbf{x} = \mathbf{x}_K$ and $\mathbf{g} = \mathbf{g}_K$.

In an interval of time $\sim \max(\text{Re } \lambda_{i>1})^{-1}$, the fast variables $y_{i>1}$ approach their quasistationary values (33) for a given y_1 and then the slow deterministic motion of y_1 is described by the equation

$$\begin{aligned} \dot{y}_1 = & -d\Xi_K(y_1)/dy_1, \quad y_1 = (y_1)_{\text{det}}, \\ \Xi_K(y) = & \frac{1}{4}a_4 y^4 + \frac{1}{2}a_2 y^2 + a_1 y, \end{aligned} \quad (48)$$

where

$$\begin{aligned} a_4 = & -f_{1111}^{(3)} - 2 \sum_{i>1} f_{11i}^{(2)} f_{11i}^{(2)} / \lambda_i \quad (a_4 > 0), \\ a_1 = & - \sum_k f_{1k}^{(0)} \delta g_k, \\ a_2 = & - \sum_k \left(f_{11k}^{(1)} + 2 \sum_{i>1} \frac{f_{ik}^{(0)} f_{11i}^{(2)}}{\lambda_i} \right) \delta g_k. \end{aligned} \quad (49)$$

In contrast to the case of a marginal bifurcation point considered above, in the vicinity of a spinode point, the fast variables influence "back" the motion of the slow one by renormalizing the coefficients in Eq. (49).

The function $\Xi_K(y)$ is a fourth-order polynomial, and for $a_4 > 0$, it can have one or two minima that correspond to the stable states of the system. For $a_2 = a_1 = 0$, the minima and the local maximum between them merge together, and this is just the spinode bifurcation point. For a given a_4 , the interrelation between the parameters a_1 and a_2 for the case where one of the minima merges with the local maximum is of the form

$$a_1^{(M)}(a_2) = \pm a(a_2), \quad a(a_2) = 2(-a_2)^{3/2} / (27a_4)^{1/2}. \quad (50)$$

Equation (50) describes the saddle-node bifurcation lines on the plane (a_1, a_2) near a spinode point sketched in Fig. 1 (both a_1 and a_2 are combinations of the control parameters of the system measured from the spinode point taken as the origin).

The analysis of the optimal paths in the vicinity of a spinode point is completely similar to that in the vicinity of a marginal point. Here too, the optimal path for \mathbf{y} is just the time-inversed deterministic path [Eqs. (47) and (48)]. The resulting expression for the action in the vicinity of a spinode point s_K is of the form

$$\begin{aligned} s_K(\mathbf{y}) = & 2F_{11}^{-1} \Xi_K(y_1) + \frac{1}{2} \sum_{i,j>1} A_{ij} [y_i - y_i^{(\text{ad})}(y_1)] \\ & \times [y_j - y_j^{(\text{ad})}(y_1)], \end{aligned} \quad (51)$$

where the matrix \hat{A} is calculated for the values of the parameters corresponding to the spinode point. In contrast to the cases considered above, s_K does not vanish in a particular stable state. Instead Eqs. (7), (10), and (51) describe the stationary (not quasistationary only) statistical distribution in the range where two stable states are close to each other and the probabilities of the transitions between them can be comparatively high (we have dropped an additive constant in s_K that allows for proper normalization of the statistical distribution).

The function s_K [Eq. (51)] is parabolic in the fast variables (the statistical distribution is Gaussian with respect to them near the maximum), whereas its dependence on the slow variable y_1 is substantially nonparabolic and the distribution over y_1 is non-Gaussian. For $a_1 = a_2 = 0$, the dependence of s_K on y_1 near the global minimum, i.e., near the stable state, is of the form of y_1^4 . In the range

$$-a(a_2) < a_1 < a(a_2), \quad a_2 < 0, \quad (52)$$

the system has two coexisting stable states and the function $\Xi_K(y_1)$ has two minima. To analyze the dependence of s_K on y_1 in this range, it is convenient to write it in the scaled form

$$\begin{aligned} s_K(y_1, y_2^{(\text{ad})}, y_3^{(\text{ad})}, \dots) = & 2F_{11}^{-1} a_2^2 a_4^{-1} \xi_K((-a_4/a_2)^{1/2} y_1, \Delta_K), \\ \xi_K(y, \Delta_K) = & \frac{1}{4}y^4 - \frac{1}{2}y^2 + y\Delta_K, \quad \Delta_K = a_1 a_4^{1/2} / (-a_2)^{3/2}. \end{aligned} \quad (53)$$

The function ξ_K is the scaled effective thermodynamic potential with respect to the scaled variable y_1 . It contains one parameter only, Δ_K . Its value determines the depths \mathcal{D}_n , $n=1$ and 2, of the minima of ξ_K which are equal to the differences between the values of ξ_K in its local maximum and the n th minimum. The values of $2F_{11}^{-1} a_2^2 a_4^{-1} \mathcal{D}_{1,2}$ give the characteristic activation energies of the transitions from the corresponding stable states.

For small $|\Delta_K|$, both minima have nearly the same depths

$$\mathcal{D}_{1,2} \approx \frac{1}{4} \mp \Delta_K, \quad |\Delta_K| \ll 1. \quad (54)$$

This means that the populations of both coexisting stable states are nearly equal for small $|\Delta_K|$, i.e., the line $\Delta_K = 0$ is the "phase-transition line" in the parameter space.

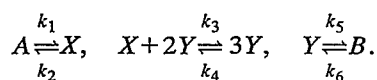
On the contrary, for $|\Delta_K|$ approaching $2/3\sqrt{3}$, i.e., for the parameter values approaching the bifurcation line (50), one of the minima becomes extremely shallow. The dependence of its depth $\mathcal{D} \approx 4 \times 3^{-5/4} (2 \times 3^{3/2} - |\Delta_K|)^{3/2}$ on the distance to the bifurcation point follows the $\frac{3}{2}$ power

law characteristic for a marginal point [cf. Eq. (45)]; the depth of the other minimum of ξ_K approaches 3/4.

VI. NUMERICAL ANALYSIS

In this section, we apply the eikonal approximation to solve for the stationary distribution of the master equation for two problems in chemical kinetics—a spatially homogeneous Selkov model and the iodate arsenous acid reaction run in two mass-coupled stirred tank reactors. Both systems are described by two variables, both systems have nonlinear rate kinetics and exhibit two stable stationary states for the parameter values chosen, and both systems lack detailed balance. The solution to the Selkov model is discussed in more detail to show explicitly how the method is applied. We obtain the stationary solution to the master equation for both models by Monte Carlo simulations as well and show the agreement of the theory and simulations.

The Selkov model is given by the chemical reaction scheme



The concentrations of species A and B , denoted by a and b , respectively ($a=A/\Omega$ and $b=B/\Omega$), are held constant; and the concentrations of the intermediate species X and Y , denoted by x and y , respectively ($x=X/\Omega$ and $y=Y/\Omega$), may vary. The concentration and corresponding generalized momentum vectors in Eq. (9) are hence two-dimensional: $\mathbf{x}=(x,y)$ and $\mathbf{p}=(p_x,p_y)$. For the values of parameters used $k_1a=106.08$, $k_2=1.16$, $k_3=0.0016$, $k_4=0.00022$, $k_5=2.0$, and $k_6b=5.17$, the deterministic equations (3) yield two stable stationary states and a saddle point (unstable stationary state). Steady state 1 is located at $(x,y)_{st}^{(1)}=(90.00,3.43)$, steady state 2 is located at $(x,y)_{st}^{(2)}=(39.87,32.50)$, and the saddle point is located at $(x,y)_s=(69.02,15.59)$. The transition probability rates $w(\mathbf{x},\mathbf{r})$ occurring in Eq. (9) are nonzero only when \mathbf{r} takes on one of the six values $(r_x,r_y)=(1,0)$, $(-1,0)$, $(-1,1)$, $(1,-1)$, $(0,-1)$, or $(0,1)$ corresponding to the six possible reactions. For $\mathbf{r}=(-1,1)$, e.g., the transition probability rate is $w[(x,y),(-1,1)]=k_3xy^2$ as terms of order $(1/\Omega)$ are neglected.

The calculation of the logarithm of the stationary solution to the master equation is started by setting the initial concentrations x and y near to one of the steady state values (a state n , $n=1$ and 2) and approximating the corresponding values of $p_x(x,y)$, $p_y(x,y)$, and $s_n(x,y)$ at that point by a Gaussian approximation of the distribution about the steady state as determined by Eqs. (12) and (13). For the calculations discussed here, the distance in concentration space of the initial points (x,y) from the steady state is 0.01.

The set of Eqs. (14) for the time evolution of $x(t)$, $y(t)$, $p_x(t)$, and $p_y(t)$ is then integrated to yield what we have called the optimal fluctuational path of the system, i.e., the path the system most likely takes in fluctuating away from the steady state. The value of $s_n(x,y)$ is calculated along this path using Eq. (15), which gives to the lowest order in Ω^{-1} the negative logarithm of the quasistationary distribution of the assumed form $P_n(X,Y)=C^{(n)} \exp[-\Omega s_n(x,y)]$.

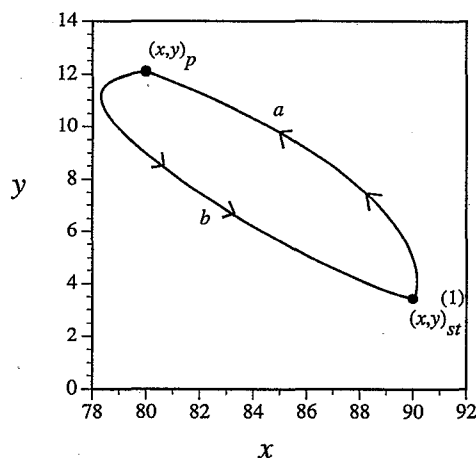


FIG. 2. (a) An optimal fluctuational trajectory leading from the steady state at $(x,y)_{st}^{(1)}=(90.03,3.43)$ to the point $(x,y)_p=(80.0,12.1)$; (b) the deterministic trajectory returning to the steady state.

Figure 2 illustrates an optimal path the system takes in fluctuating from the vicinity of steady state 1 to a given point [the point $(x,y)=(80.0,12.1)$] as well as the deterministic trajectory from the given point back to the steady state. It can be seen in the figure that in the absence of detailed balance, the optimal path differs from the deterministic path.

Calculations of optimal fluctuational paths are repeated for different initial points (x,y) surrounding the steady state at the same distance. As the optimal trajectories starting at different points lead to different areas of the concentration space, the values of $s_n(x,y)$ can be mapped over the concentration plane. The procedure of calculating trajectories and the value of $s_n(x,y)$ along these optimal trajectories is then repeated using initial points $(x$ and $y)$ surrounding the other steady state. For all calculations, the value of $s_n(x,y)$ at the steady state is taken to be 0.

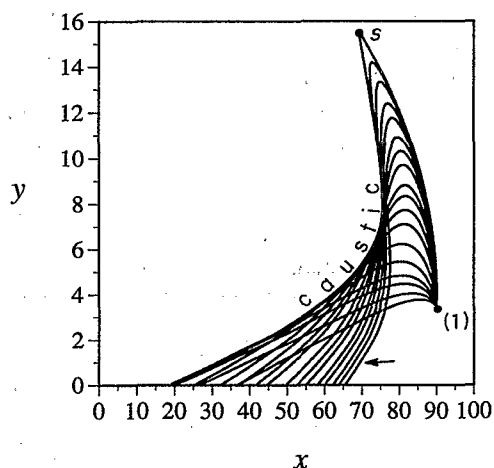


FIG. 3. Optimal fluctuational paths emanating from the stable stationary state $(x,y)_{st}^{(1)}=(90.03,3.43)$ marked (1) in the concentration plane (x,y) for the Selkov model. The caustic is indicated and the arrow points to the limiting trajectory. s denotes the saddle point.

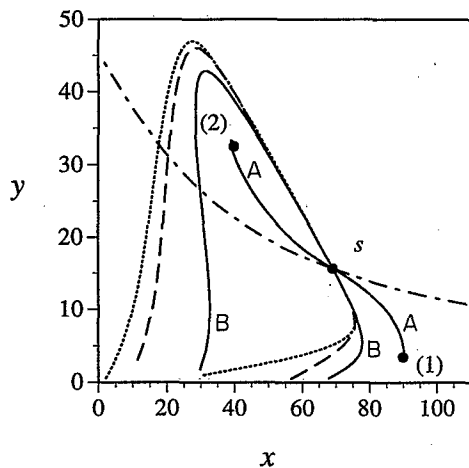


FIG. 4. Features of the concentration plane (x, y) for the Selkov model. The symbols denote the following: solid lines marked A denote limiting fluctuational trajectories from stable stationary states (1) and (2) to the saddle point s ; solid lines marked B denote the continuation of the limiting trajectories from the saddle point region; dotted lines denote the caustics; the dashed line denotes the fluctuational separatrix which is the locus of points reached with equal probability, by a fluctuation from either stationary state; the dotted-dashed line denotes the deterministic separatrix.

A qualitative feature of the calculations, illustrated in Fig. 3, is the presence of a caustic bounding the region of concentration space $[x(t), y(t)]$ accessible to the optimal fluctuational paths originating at a given stable stationary state. Another caustic associated with the optimal fluctuational paths from the other steady state is present as well. While the optimal paths start at the stable stationary states, these caustics emanate from the saddle point and are shown as the dotted lines in Fig. 4. For systems described by Fokker-Planck equations, the caustics emanating from a saddle point have been found numerically by Chinarov *et al.*^{10(b)}

Suppose one scans through all initial points (x, y) at the same small concentration "distance" (e.g., 0.01) from one of the stable stationary states. For some specific initial condition, an optimal fluctuational path will be found that leads to the saddle point. As initial points approach that specific starting value from either side, the resulting optimal fluctuational paths will approach the limiting path, each of which first coincides with the path to the saddle point (curves A in Fig. 4) and then deviates away from it (curves B in Fig. 4). From the vicinity of the saddle point onward, the limiting paths associated with each stable stationary point coincide with each other. A distinction needs to be made—the caustics (in fact, the switching lines emanating from the saddle point in addition to caustics²⁹) bound the concentration space accessible via optimal fluctuational paths from a stationary state; the limiting paths from each stable stationary state bound the behavior of optimal fluctuational paths as their initial conditions approach those associated with the path to the saddle point.

A topological perspective may provide additional insight.²⁹ The limiting path is the projection of the "cut" of the manifold formed by the paths emanating from a given

fixed point. The cuts for the two manifolds that correspond to the two coexisting stable states coincide with each other. It is straightforward to evaluate the form of the cut in the vicinity of the saddle point by linearizing Eqs. (14). The caustics (the projections of the folds) of these manifolds lie on the opposite sides of the saddle point.

From the definition of the cut as a limiting trajectory, the values of the action $s_1(x, y)$ and $s_2(x, y)$ on opposite sides of the cut differ by a constant which is equal to the difference of s_1 and s_2 at the saddle point. In the limit of large Ω , the logarithm of the stationary probability distribution $P(X, Y)$ is given by the continuous function $s(x, y)$. This function is determined on balance, so that the probability to reach the saddle point from state 1, weighted with its occupation w_1 is equal to logarithmic accuracy to that from state 2 weighted with its occupation w_2 . In enumerating the states, we assume that $s_1(x_s, y_s) > s_2(x_s, y_s)$, and thus state 1 is occupied predominantly: $w_1/w_2 \propto \exp\{\Omega[s_1(x_s, y_s) - s_2(x_s, y_s)]\} \gg 1$. Then,

$$\Omega^{-1} \ln P(X, Y) = -s(x, y), \quad (55)$$

$$s(x, y) = \min \left\{ \begin{array}{l} s_1(x, y), \\ s_2(x, y) + s_1(x_s, y_s) - s_2(x_s, y_s). \end{array} \right.$$

It is clear from Fig. 3 that the paths $(x(t), y(t))$ emanating from one stationary state may intersect each other in the range between the caustic and the limiting path. It is also possible to reach this region on an optimal fluctuational trajectory from the other stationary state. (An approximation including multiple path contributions to the total probability of observing the system in this vicinity of concentration space is worthy of consideration, by analogy with standard semiclassical techniques.) It is in this area that the line $s_1(x, y) = s_2(x, y) + s_1(x_s, y_s) - s_2(x_s, y_s)$ lies. This line can be reasonably called the fluctuational separatrix (cf. Refs. 29 and 30) and is shown as the dashed line in Fig. 4 for the Selkov model. It separates the concentration plane into two regions; each region corresponds to concentrations the system attains having most likely fluctuated from one or the other stable state. The fluctuational separatrix consists of two branches which start at the saddle point. It does not coincide, however, with the deterministic separatrix (the dotted-dashed line in Fig. 4) that separates the ranges of the deterministic motion down to one or the other stable state. Thus the regions of phase space to which a system arrives from a given stable state as a result of large fluctuations do not coincide with the regions from which the system approaches the same stable state along deterministic paths.

To check the validity of the function $P^{(n)}(X, Y) = C^{(n)} \exp[-\Omega s_n(x, y)]$ obtained with the eikonal approximation as a solution to the stationary master equation, the calculated values of $P^{(n)}(X, Y)$ for a given point (x, y) in concentration space for varying system sizes are substituted back into the right-hand side of the master equation (1) and divided by $P^{(n)}(X, Y)$. The value of the ratio {i.e., formally $(\partial P^{(n)}/\partial t)/P^{(n)}$ } ought to be independent of the system size, and at the point $(x, y) = (50, 23)$, a point not near a steady state, this ratio has the values $-0.26, -0.72, 0.85,$ and 1.61 for $\Omega = 1, 10^2, 10^3,$ and 10^4 , respectively. As expected, it is

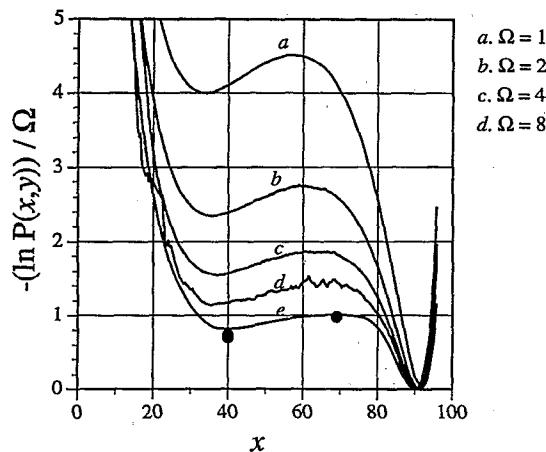


FIG. 5. Monte Carlo calculations of the scaled logarithm of the stationary probability distribution for the Selkov model along the straight line connecting the two stable steady states plotted against the value of x along this line for (a) $\Omega=1$; (b) $\Omega=2$; (c) $\Omega=4$; and (d) $\Omega=8$. (e) The eikonal approximation to this quantity valid in the limit of large systems. The marks at $x=39.87$ and at $x=69.02$ are extrapolations of the Monte Carlo simulations for infinite system size as explained in the text.

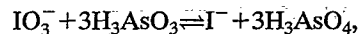
nearly independent of the system size as the system size increases several orders of magnitude, and this indicates the validity of the obtained solution in regions even far from the steady states. The deviation of the eikonal approximation from the exact solution is due to the neglect of higher order terms in the reciprocal system size Ω^{-1} , which give rise to the preexponential factor in the solution which depends on x and y . An additional error in the numerical result comes from the initial values of p_x and p_y not being small enough for a given Ω , i.e. from not starting the trajectories near enough to the stable steady state.

The stationary solution to the master equation for the Selkov model is also obtained by performing Monte Carlo simulations using the method outlined by Gillespie.³¹ The random number generator used is G05CAF of the NAG FORTRAN Library Mark 15 and has a period of 2^{57} . The simulation involves following the reacting system in time and keeping track of how much time it spends in each state (X,Y) . The system is followed for up to 2 billion reaction steps. The probability distribution obtained from these simulations is normalized so that the most probable state has a probability of exactly 1, the same normalization we used for calculating the stationary distribution. We perform simulations for four different system sizes $\Omega=1, 2, 4$, and 8 in which the number of X and Y particles in steady state 1 are $(X,Y) \sim (90,3), (180,6), (360,12)$, and $(720,24)$ respectively.

In Fig. 5, we plot the values of $-\ln P(X,Y)/\Omega$ obtained by the Monte Carlo simulations along the straight line $y(x)$ connecting the two deterministic stable states against the value of x along this line, as well as the eikonal approximation to this quantity. This line runs very near to the saddle point as well. In the limit of large systems, the values of $-\ln P(X,Y)/\Omega$ obtained from Monte Carlo simulations for differing system sizes are expected to coincide with each other. As can be seen from the graph, the Monte Carlo solu-

tion as a whole approaches the theoretically calculated solution as the system size increases. When the values of $-\ln P(X,Y)/\Omega$ are plotted against $1/\Omega$ for a chosen point (x,y) , the plot is nearly linear. The values of $-\ln P(X,Y)/\Omega$ at $1/\Omega=0$ are linearly extrapolated for two values of $x,y(x)$ (corresponding to the less probable steady state and to a point very near the saddle) and are shown on the figure by dark marks. The spread of the marks gives an estimate of the error of the Monte Carlo extrapolation. The agreement of the eikonal approximation and the Monte Carlo simulations is quite good for the Selkov model.

The second problem we solve is for the stationary distribution of the master equation corresponding to the iodate arsenous acid reaction taking place in two diffusively coupled continuously stirred flow reactors. The reaction occurring in each tank³² is



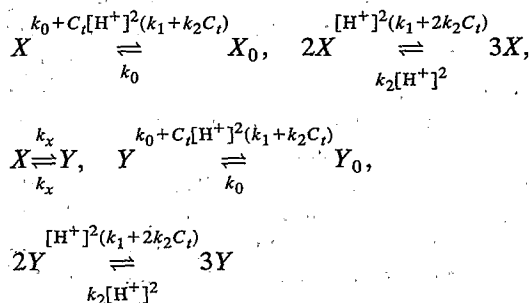
where iodate (IO_3^-) and arsenous acid (H_3AsO_3) are flowed separately into each tank and the acid concentration is in large excess of the iodate concentration. The reactors are coupled to each other and chemical species can exchange between the reactors through linear diffusion.

We let X and Y represent the iodate species in reactors 1 and 2, respectively. The equations governing the reaction, flow, and exchange processes after initial transients have decayed are³²

$$\begin{aligned} \frac{dX}{dt} &= -[k_1 + k_2(C_t - X)](C_t - X)X[\text{H}^+]^2 \\ &\quad + k_0(X_0 - X) + k_x(Y - X), \\ \frac{dY}{dt} &= -[k_1 + k_2(C_t - Y)](C_t - Y)Y[\text{H}^+]^2 \\ &\quad + k_0(Y_0 - Y) + k_x(X - Y), \end{aligned} \quad (56)$$

where k_1 and k_2 are experimentally determined rate coefficients describing the homogeneous chemical kinetics, k_0 is the reciprocal residence time of species in a reactor, k_x is a measure of the coupling between the reactors, X_0 and Y_0 are the inflow concentrations of iodate to reactors 1 and 2, respectively, and C_t is the concentration of the all species containing iodine in each reactor, i.e., $C_t = [\text{IO}_3^-] + [\text{I}^-]$ in each tank after transients have decayed. The acid concentration in each tank $[\text{H}^+]$ is taken to be in large excess of $[\text{IO}_3^-]$ and is considered a constant.

The following "chemical mechanism:"



consisting of five reversible reactions with the given expressions as rate constants can be written to describe the kinetics

of the system of interest.³³ The deterministic equations derived from the reaction scheme are Eqs. (56), and the transition probabilities $w(x,r)$ arising in the master equation are derived from this mechanism as well.

We use the dimensional parameter values $k_1=4.5\times 10^3$ $M^{-3}s^{-1}$, $k_2=4.5\times 10^8$ $M^{-4}s^{-1}$, $k_0=7.25\times 10^{-3}$ $M s^{-1}$, $k_x=2.0\times 10^{-3}$ $M s^{-1}$, $X_0=0.98\times 10^{-3}$ M , $Y_0=1.02\times 10^{-3}$ M , $[H^+]=7.55\times 10^{-3}$ M , and $C_i=1.0441\times 10^{-3}$ M . This system has two stable steady states (both nodes) and a saddle point located at the concentrations $(x,y)_{st}^{(1)}=(3.92\times 10^{-4}, 4.25\times 10^{-4})$ M , $(x,y)_{st}^{(2)}=(9.67\times 10^{-4}, 10.03\times 10^{-4})$ M , and $(x,y)_s=(6.34\times 10^{-4}, 7.81\times 10^{-4})$ M .

The procedure of calculating the logarithm of the probability distribution $P(X,Y)$ is the same as that used in evaluating the distribution of the Selkov model. We calculate various optimal trajectories emanating from each steady state, calculate $s_n(x,y)$ along these trajectories, and match the solutions. The offset value added to the values of $s_2(x,y)$ obtained from trajectories emanating from the less stable state $(x,y)_{st}^{(2)}$ is 2.04×10^{-4} . We again choose the normalization so that the integral over the vicinity of the most probable state $(x,y)_{st}^{(1)}$ is equal to 1.

To check the obtained solution, we substitute the solution into the master equation and calculate the ratio of the right-hand side to P [i.e., formally the quantity $(\partial P/\partial t)/P$] at a point not near a stable steady state for increasing values of Ω . The point chosen is $(x,y)=(5.0\times 10^{-4}, 6.7\times 10^{-4})$ M . The values of the ratio are equal to 4.9×10^{-4} , 7.9×10^{-4} , 1.3×10^{-3} , 1.7×10^{-3} , and 6.3×10^{-3} for $\Omega=10^5$, 10^6 , 10^7 , 10^8 , and 10^9 , respectively. As the system size increases orders of magnitude, the ratio remains largely independent of the system size as expected, and this fact indicates the validity of the obtained solution.

We also perform Monte Carlo simulations³¹ of the "chemical mechanism" of interest for three system sizes $\Omega=4\times 10^5$, 8×10^5 , and 16×10^5 for which the numbers of particles in the steady state 1 are roughly $(X,Y)_{st}^{(1)}\sim(160,160)$, $(320,320)$, and $(640,640)$, respectively; and we follow the chemical system for up to 2 billion reaction steps. Figure 6 displays the results of the three Monte Carlo simulations along with the theoretical solution. Again, the values of the scaled logarithm of the probability distribution $-\ln P(X,Y)/\Omega$ along the straight line $y(x)$ connecting the two deterministic stable steady states are shown as a function of the variable x along this line. Even though the simulations give a rough curve, the approach of the Monte Carlo simulations to the theoretical result is apparent with increasing Ω . The isolated marks on the figure near the minimum of $P[X,Y(X)]$ and at the less probable stable state are the estimates of where the Monte Carlo simulations are converging from the same type linear extrapolation as used in the Monte Carlo simulations of the Selkov model.

While optimal fluctuational trajectories offer several advantages, there are also a few disadvantages in having to calculate them first in order to obtain the stationary solution to the master equation. The first inconvenience is that given a point (x,y) , one does not know *a priori* which initial conditions will give a trajectory which leads to the vicinity of the desired point. One must simply calculate some trajecto-

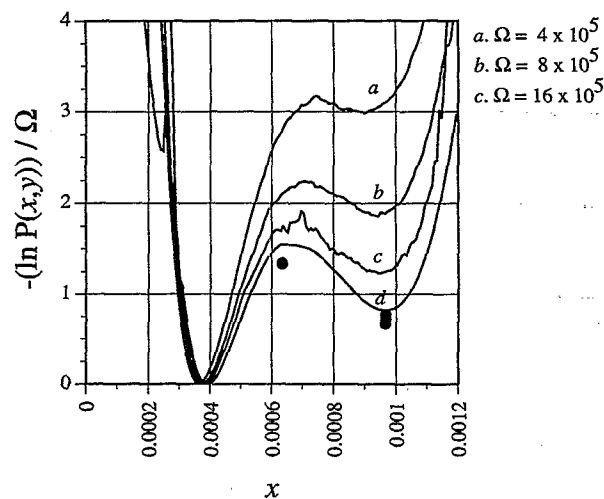


FIG. 6. Monte Carlo calculations of the scaled logarithm of the stationary probability distribution for the iodate arsenous acid reaction in coupled reactors along the straight line connecting the two stable steady states plotted against the value of x along this line for (a) $\Omega=4\times 10^5$; (b) $\Omega=8\times 10^5$; and (c) $\Omega=16\times 10^5$. (d) The eikonal approximation to this quantity valid in the limit of large systems. The marks at $x=6.34\times 10^{-4}$ and at $x=10.03\times 10^{-4}$ are extrapolations of the Monte Carlo simulations for infinite system size as explained in the text.

ries with varying initial conditions and see where they lead. Another potential difficulty is that if the trajectories tend to move strongly in one direction vs another, it may be difficult to calculate numerically desired trajectories which follow the less favored direction.

VII. CONCLUSIONS

The instanton approach to the problem of large occasional fluctuations in noise-driven dynamical systems⁴⁻¹⁶ makes it possible to reduce, to logarithmic accuracy, the evaluation of the density distribution of chemical species in a homogeneous reactor to a problem of Hamiltonian mechanics of an auxiliary system. Both auto- and nonautocatalytic reactions, and both reactions with and without detailed balance can be described this way. The Hamiltonian of the auxiliary system can be expressed in terms of the probabilities of elementary reactions between the species involved, i.e., in terms of the chemical reaction rates. The logarithm of the statistical distribution of a chemical system is proportional to the mechanical action of the auxiliary dynamical system, and this action is a Liapunov function. The logarithm of the probability of escape from a metastable stationary state is determined by the action evaluated between this state and the saddle point in the space of the variables (the densities of the species). These are the escape probabilities that give, on balance, the stationary distribution over coexisting stable states. To the lowest order in the reciprocal volume of the system, the logarithm of the stationary distribution is a nonanalytic function of the densities of the species, in the general case, and special care has to be taken to describe it.

The explicit expressions for the logarithm of the statistical distributions and for the escape probabilities have been obtained for several types of systems—systems with detailed

balance, one-species systems (including these without detailed balance), and systems close to a bifurcation point. In the latter case, the fluctuations display universal behavior. In particular, near a saddle-node bifurcation point, the logarithm of the probability of escape from a metastable state scales like the distance to the bifurcation point to the power $3/2$. A simple scaling law also holds in the vicinity of a spinode bifurcation point where two stable stationary states merge with an unstable one. Not only quasistationary statistical distribution about a stable stationary state, but also global stationary distribution can be obtained explicitly in this case, and the phase transition line is obtained where the populations of the both stable states are equal in order of magnitude.

In prior theoretical work on the formulation of a thermodynamic and stochastic theory of nonlinear physical and chemical systems, there appears an excess work.^{17,18,34} This excess work is a Liapunov function for the deterministic relaxation towards stationary states; an affinity towards a stationary state; a function that yields necessary and sufficient conditions of stability; a component of the total dissipation; and, in the case of systems with detailed balance, a state function and a solution to the stationary master equation for chemical systems. For nonlinear systems lacking detailed balance, the excess work is no longer a state function and a path of integration from a stationary state $(x,y)_{st}^{(n)}$ to an arbitrary state (x,y) needs to be specified.

For a fluctuation from $(x,y)_{st}^{(n)}$ to (x,y) , the reverse of the deterministic path from (x,y) to $(x,y)_{st}^{(n)}$ was chosen in Ref. 34. This choice was tested on the Selkov model for given parameters and found to provide a solution to the stationary probability density. For that choice of parameters for the Selkov model, the eikonal approximation could not be evaluated numerically. Both results are due likely to very different time scales for the X and Y motion for that problem.

For the choices of parameters of the Selkov model used for the results in Fig. 5, the excess work evaluated along the reverse of the deterministic trajectory yields a probability distribution with inverted peak heights as those given by the eikonal approximation and the Monte Carlo simulations. A similar result is obtained for the two-tank iodate arsenous acid problem. The use of the reverse deterministic path in the evaluation of the excess work does not yield a stationary solution of the master equation if there is lack of detailed balance.

In spatially nonuniform systems, the choice of the deterministic trajectory in the evaluation of the excess work for the calculation of relative stability yields results identical to solutions of deterministic reaction-diffusion equations.³⁵ The method of solution of stochastic equations for inhomogeneous systems, in part for analysis of relative stability to be compared with experiments, needs yet to be developed.

ACKNOWLEDGMENTS

We thank Professor Katharine L. C. Hunt, Professor P. V. E. McClintock, Dr. M. Millonas, Dr. Bo Peng, and Dr. V. N. Smelyanskiy for helpful discussions. This work was sup-

ported in part by the Department of Energy/BES Engineering Program.

- ¹(a) H. Haken, *Synergetics. An Introduction*, 2nd ed. (Springer, New York, 1978); (b) N. G. van Kampen, *Stochastic Processes in Physics and Chemistry* (North Holland, New York, 1981).
- ²C. W. Gardiner, *Handbook of Stochastic Methods*, 2nd ed. (Springer, New York, 1990).
- ³H. A. Kramers, *Physica (Utrecht)* **7**, 240 (1940).
- ⁴A. D. Wentzell and M. I. Freidlin, *Russ. Math. Surveys* **25**, 1 (1970); M. I. Freidlin and A. D. Wentzell, *Random Perturbations in Dynamical Systems* (Springer, New York, 1984).
- ⁵D. Ludwig, *SIAM Rev.* **17**, 605 (1975).
- ⁶B. J. Matkowsky and Z. Schuss, *SIAM J. Appl. Math.* **33**, 365 (1977); (b) Z. Schuss and B. J. Matkowsky, *ibid.* **35**, 604 (1979); B. J. Matkowsky and Z. Schuss, *Physica (Utrecht) A* **95**, 213 (1983).
- ⁷M. I. Dykman and M. A. Krivoglaz, *Sov. Phys. JETP* **50**, 30 (1979).
- ⁸(a) R. Graham and A. Schenzle, *Phys. Rev. A* **23**, 1302 (1981); R. Graham and T. Tel, *Phys. Rev. A* **31**, 1109 (1985); **33**, 1322 (1986); (b) R. Graham, in *Noise in Nonlinear Dynamical Systems*, edited by F. Moss and P. V. E. McClintock (Cambridge University, Cambridge, 1989), Vol. 1, p. 225.
- ⁹E. Ben-Jacob, D. J. Bergman, B. J. Matkowsky, and Z. Schuss, *Phys. Rev. A* **26**, 2805 (1982); R. L. Kautz, *Phys. Rev. A* **38**, 2066 (1988).
- ¹⁰(a) R. S. Maier and D. L. Stein, *Phys. Rev. Lett.* **69**, 3691 (1992); (b) V. A. Chinarov, M. I. Dykman, and V. N. Smelyanskiy, *Phys. Rev. E* **47**, 2448 (1993).
- ¹¹J. F. Luciani and A. D. Verga, *Europhys. Lett.* **4**, 255 (1987); M. M. Klosek-Dygas, B. J. Matkowsky, and Z. Schuss, *SIAM J. Appl. Math.* **48**, 425 (1988); A. J. Bray and A. J. McKane, *Phys. Rev. Lett.* **62**, 493 (1989); A. J. Bray, A. J. McKane, and T. J. Newman, *Phys. Rev. A* **41**, 657 (1990).
- ¹²M. I. Dykman, *Phys. Rev. A* **42**, 2020 (1990); M. I. Dykman, P. V. E. McClintock, N. D. Stein, and N. G. Stocks, *Phys. Rev. Lett.* **67**, 933 (1991); M. I. Dykman, R. Mannella, P. V. E. McClintock, N. D. Stein, and N. G. Stocks, *Phys. Rev. E* **47**, 3996 (1993).
- ¹³(a) B. J. Matkowsky, Z. Schuss, C. Knessl, C. Tier, and M. Mangel, *Phys. Rev. A* **29**, 3359 (1984); C. Knessl, M. Mangel, B. J. Matkowsky, Z. Schuss, and C. Tier, *J. Chem. Phys.* **81**, 1285 (1984); C. Knessl, B. J. Matkowsky, Z. Schuss, and C. Tier, *J. Stat. Phys.* **42**, 169 (1986); (b) Hu Gang, *Z. Phys. B* **65**, 103 (1986); *Phys. Rev. A* **36**, 5782 (1987).
- ¹⁴R. Reimann and P. Talkner, *Phys. Rev. A* **44**, 6348 (1991); A. Hamm and R. Graham, *J. Stat. Phys.* **66**, 689 (1991).
- ¹⁵A. D. Wentzell, *Theory Prob. Its Appl.* **21**, 227 (1976); **21**, 499 (1976).
- ¹⁶R. S. Maier, *Random Struct. Algorithms* **2**, 379 (1991); *Proceedings of the 1992 Complex Systems Summer School* (Addison-Wesley, New York, 1992).
- ¹⁷P. M. Hunt, K. L. C. Hunt, and J. Ross, *J. Chem. Phys.* **92**, 2572 (1990).
- ¹⁸P. M. Hunt, K. L. C. Hunt, and J. Ross, *J. Chem. Phys.* **96**, 618 (1991).
- ¹⁹L. D. Landau and E. M. Lifshitz, *Statistical Physics*, 3rd ed. (Pergamon, New York, 1980), Part 1.
- ²⁰R. Kubo, K. Matsuo, and K. Kitahara, *J. Stat. Phys.* **9**, 51 (1973); K. Kitahara, *Adv. Chem. Phys.* **29**, 85 (1973).
- ²¹L. D. Landau and E. M. Lifshitz, *Mechanics* (Pergamon, London, 1976).
- ²²H. Risken, *The Fokker-Planck Equation*, 2nd ed. (Springer, Berlin, 1989).
- ²³L. E. Reichl, Z.-Y. Chen, and M. M. Millonas, *Phys. Rev. Lett.* **63**, 2013 (1989); *Phys. Rev. A* **41**, 1874 (1990).
- ²⁴K. L. C. Hunt, P. M. Hunt, and J. Ross, *Annu. Rev. Phys. Chem.* **41**, 409 (1990).
- ²⁵R. Landauer, *J. Appl. Phys.* **33**, 2209 (1962).
- ²⁶V. Arnold, *Ordinary Differential Equations*, 3rd ed. (Springer, Berlin, 1992).
- ²⁷M. I. Dykman and M. A. Krivoglaz, *Physica (Utrecht) A* **104**, 480 (1980); in *Soviet Physics Reviews*, edited by I. M. Khalatnikov (Harwood, New York, 1984), Vol. 5, p. 261.
- ²⁸K. Wiesenfeld, in *Noise in Nonlinear Dynamical Systems*, edited by F. Moss and P. V. E. McClintock (Cambridge University, Cambridge, 1989), Vol. 2, p. 145.
- ²⁹V. N. Smelyanskiy, M. I. Dykman, and M. Millonas, in *Fluctuations and Order: a New Synthesis* (Springer, Berlin, 1994).
- ³⁰M. I. Dykman, R. Mannella, P. V. E. McClintock, and N. D. Stein (to be published).
- ³¹D. T. Gillespie, *J. Phys. Chem.* **81**, 2340 (1977); *J. Comp. Phys.* **22**, 403 (1976).

- ³²S. Dushman, *J. Phys. Chem.* **8**, 453 (1904); H. A. Liebhafshy and G. M. Roe, *Int. Chem. Kinet.* **11**, 693 (1983); N. Ganapathisubramanian and K. Showalter, *J. Phys. Chem.* **87**, 1098 (1983).
- ³³K. L. C. Hunt and B. Peng (private communication, 1993).
- ³⁴J. Ross, K. L. C. Hunt, and P. M. Hunt, *J. Chem. Phys.* **96**, 618 (1992); Q. Zheng, J. Ross, K. L. C. Hunt, and P. M. Hunt, *ibid.* **96**, 630 (1992).
- ³⁵X.-L. Chu, P. M. Hunt, K. L. C. Hunt, and J. Ross, *J. Chem. Phys.* (to be published).